Applied Magnetic Resonance (2022) 53:1105–1119
https://doi.org/10.1007/s00723-021-01428-w

Applied
Magnetic Resonance

ORIGINAL PAPER

Pitfalls in Sample Preparation of Metalloproteins for Low-Temperature EPR: The Example of Alkaline Myoglobin

Ilenia Serra[1,2] · Inés García Rubio[2,3] · Sabine Van Doorslaer[1]

Received: 30 April 2021 / Revised: 2 September 2021 / Accepted: 6 September 2021 /
Published online: 23 September 2021

Abstract

Due to fast relaxation processes of transition metal ions, electron paramagnetic resonance (EPR) spectroscopy of metalloproteins needs to be performed at cryogenic temperatures. To avoid damaging the biological system upon freezing, a cryoprotectant is generally added to the sample as a glassing agent. Even though cryoprotectants are expected to be inert substances, evidences in literature show their non-innocent role in altering the shape of EPR spectra of proteins and biological objects in general. In this work we conduct a systematic study on the impact of several experimental factors—such as buffer composition, choice of cryoprotectant, pH and temperature—on the EPR spectrum of myoglobin, taken as a reference system for being a well-characterized heme-containing protein. We focus on high-pH buffers to induce and investigate the alkaline transition of ferric myoglobin (pKa ~ 8.9). A combined approach of continuous-wave EPR and UV–visible absorption spectroscopy shows that using particular pairs of buffers and cryoprotectants determines a considerable pH variation in the sample and that this effect is enhanced at cryogenic temperature. In addition, phase memory times were measured to evaluate the efficiency of different cryoprotectants and compared with spectral linewidths in continuous-wave EPR. Our findings suggest that among the selected cryoprotectants ethylene glycol is rather effective, even more than the widely used glycerol, without having unwanted effects.

✉ Inés García Rubio
inesgr@unizar.es

✉ Sabine Van Doorslaer
sabine.vandoorslaer@uantwerpen.be

Extended author information available on the last page of the article

1 Introduction

Metalloproteins possessing paramagnetic centres are widely investigated by electron paramagnetic resonance (EPR) spectroscopy to get insight into the spin and oxidation state of the paramagnet, as well as information on local symmetry and geometry. From a spectroscopic point of view, because of the rapid electron spin–lattice and spin–spin relaxation rates of paramagnetic transition metal-containing systems, the EPR experiment needs to be performed at cryogenic temperatures to detect a sufficiently intense and resolved signal [1].

Metalloproteins and biological samples in general are prepared and stored in aqueous media. The formation of ice crystals upon freezing represents an issue during the preparation of samples for low-temperature EPR measurements since, in addition to the risk of breaking the EPR tube, large ice crystals may damage the biological object [2] or cause a mechanical stress on the molecules causing a broader distribution of environments of the paramagnetic moiety which will result in an increased EPR linewidth (larger *g*-strain) and shortened phase memory times [1]. Moreover, the freezing process can induce the separation of the sample in a phase of pure ice crystals and another containing the concentrated solute [3], where proteins might suffer from a large variation in local concentration, ionic strength or pH. These inhomogeneities could in turn affect the EPR signal, giving rise to artefacts or poorly resolved features. To overcome these hindrances, a cryoprotectant is commonly added to the sample to prevent the formation of ice crystals promoting a homogenous glass upon freezing [4]. Glycerol is by far the most used glassing agent for EPR investigations of biological systems, but ethylene glycol, sucrose [5] and more recently trehalose [6] have been employed as well. Despite being generally considered as biologically inert, evidences of a non-innocent role of these substances can be found throughout the EPR literature of biological samples [7–13].

Heme-containing proteins are a relevant class of metalloproteins that cover an extensive range of biological functions, including oxygen transport and storage, reduction of peroxides, oxygenation of substrates and electron transfer. Notably, the key to carry out such a diversity of reactions essentially resides in a common prosthetic group, i.e. the heme, consisting of a porphyrin ring which coordinates an iron ion at its centre [14]. In these systems the iron can adopt different oxidation states, among which some are paramagnetic and suitable to be investigated by EPR spectroscopy. This technique can therefore provide valuable information on the architecture of the active site pocket, where the heme moiety is located [15, 16].

pH-dependent experiments are commonly carried out to elucidate protein behaviour, for instance with the attempt to reproduce a certain (or altered) physiological environment [17], or in applied research, to examine the performance of enzymes in sub-optimal conditions which might be necessary for industrial utilization [18]. Many heme proteins have been described to undergo an alkaline transition at high pH related to different deprotonation processes [19–23]. Here, we use the well-characterized myoglobin (Mb) as model heme protein to explore

a number of experimental setups using different alkaline buffers together with a chosen set of cryoprotectants to investigate the influence of such conditions on the EPR spectra. It is known that a high-spin to low-spin transition occurs in ferric Mb related to the deprotonation of the water molecule axially coordinated to the heme iron (pKa values of ~ 8.9 were reported previously [19, 23, 24]). The EPR spectrum of alkaline ferric Mb is characteristic of a low-spin (LS) ($S = 1/2$) heme iron, with earlier reported g values reflecting the proximal ligation of a histidine and distal ligation of a hydroxide group [19, 25, 26].

Because the impact of procedural factors on the observed EPR signal of heme proteins may lead to erroneous data interpretation, we want to draw the attention to the importance of tailoring the process of sample preparation to the investigated system. Our results demonstrate that the choice of buffer and cryoprotectant, as well as their combination, is not trivial in the design of low-temperature EPR experiments on proteins, not even for a well-known system, like myoglobin.

2 Experimental Procedures

2.1 Materials

Myoglobin from horse skeletal muscle (95–100% pure, essentially salt-free, lyophilized powder) was purchased from Sigma-Aldrich and used without further purification. Alkaline buffers (pH 9.8 to 10) boric acid–NaOH (herein referred to as borate buffer, Panreac), glycine–NaOH (glycine buffer, Sigma-Aldrich), Na_2CO_3–$NaHCO_3$ (carbonate–bicarbonate buffer, Panreac), 3-(cyclohexylamino)-1-propanesulphonic acid (CAPS, Sigma-Aldrich) and 2-(cyclohexylamino)-ethanesulphonic acid (CHES, Sigma-Aldrich) were prepared at a concentration of 0.1 M, filtered and degassed. For EPR measurements, the buffers were used at a final concentration of 0.05 M. The glassing agents glycerol, ethylene glycol and sucrose were purchased from Panreac, trehalose from Sigma-Aldrich.

2.2 Optical and EPR Spectroscopies

Myoglobin stock solutions were prepared by dissolving ~ 2 mg of lyophilized myoglobin in 100 µL of each buffer. For all solutions, protein concentration was determined spectrophotometrically with an Analytikjena Specord® 200 plus spectrometer, using 129.000 M^{-1} cm^{-1} as molar absorptivity of Mb at the Soret peak [27, 28], then samples for EPR measurements were prepared to a final concentration of 0.2 mM. For the samples containing glycerol or ethylene glycol, 20 µL of pure substance was added to 80 µL of protein solution to obtain a 20% (v/v) concentration of the cryoprotectant. In the case of sucrose and trehalose, myoglobin was dissolved in the buffer already containing the sugar at a concentration of 0.36 M. Representative concentrations of the cryoprotectants were chosen on the basis of the ones used in previous EPR studies [10, 13].

CW-EPR measurements were performed with a Bruker ELEXSYS E580 X-band spectrometer equipped either with an Oxford CF935 continuous-flow cryostat and a Bruker ER4118 SPT-N1 resonator (operating at a microwave (MW) frequency of ~ 9.7 GHz) or with an Oxford ESR 900 continuous-flow cryostat and a Bruker ER 4122 SHQ resonator (operating at a MW frequency of ~ 9.4 GHz). The spectra were taken at a temperature of 10 K with non-saturating MW powers, 1 mT of modulation amplitude and 100 kHz modulation frequency. Reported *g* values were obtained from simulations of EPR spectra performed with the Easyspin software (v. 6.0.0-dev.26) [29].

Pulse EPR experiments were performed at 10 K with an Oxford CF935 continuous-flow cryostat and a Bruker ER4118 SPT-N1 resonator operating at a MW frequency of ~ 9.7 GHz. A Hahn echo sequence $\pi/2$–τ–π–τ–*echo* with 2-step phase cycle and long pulses ($t_{\pi/2}$ ~ 50 to 96 ns) in order to minimize echo modulation was used to measure the phase memory times (T_m). A shot repetition time of 1020 µs was used and the interval between the pulses τ was varied from 148 to 3344 ns in steps of 4 ns. The T_m traces were fitted in Matlab (MathWorks, R2020b) using an exponential decay function described by the following equation:

$$f(\tau) = Ae^{-B\tau}, \tag{1}$$

where A is the amplitude and B is defined as $1/T_m$.

2.3 pH Measurements

The possible variation of pH upon addition of increasing amounts of glycerol to different buffers was monitored at room temperature (27 °C ± 0.5) with a Crison GLP 21 pH-meter. The initial pH was measured in 47.5 mL of each buffer at a concentration of 0.1 M. Aliquots of glycerol and fresh buffer were properly added to the initial volume to obtain 5, 10, 15, 20, and 30% (v/v) glycerol/buffer solutions. For each concentration point, the solution was stirred with magnetic agitation for 5 min to avoid inhomogeneities in liquid density before measuring the pH. The pH stability of the buffers was also tested with a Thermo Scientific Orion Star A111 pH-meter at room temperature (23 °C ± 0.5) in the presence of 20% (v/v) of ethylene glycol, 0.36 M of sucrose or 0.36 M of trehalose.

3 Results

3.1 EPR and UV–Visible Spectroscopy

To maintain biological samples at high pH, several well-known buffers can be used. In this study we chose borate, glycine, carbonate–bicarbonate, CAPS and CHES as exemplary buffers to have a varied set in terms of chemical composition. Being extensively used in EPR spectroscopy, glycerol was initially employed in a comparative EPR experiment, to check whether it had any influence on the high-pH spectrum of myoglobin. Figure 1 shows the CW X-band EPR spectra of myoglobin in

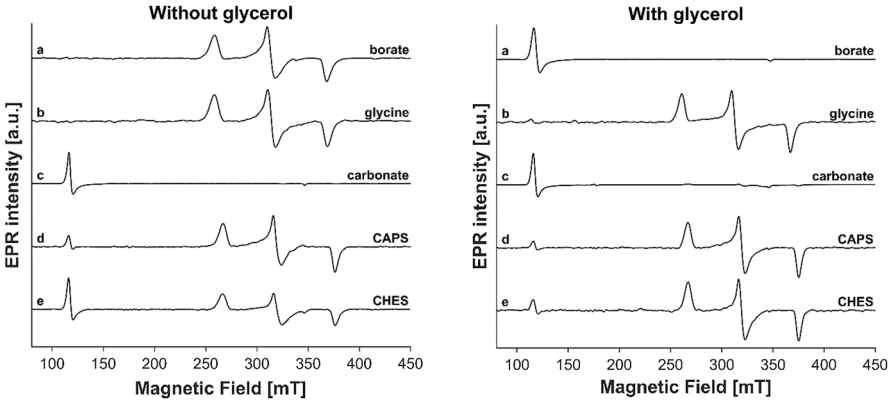

Fig. 1 X-band CW-EPR spectra of myoglobin in alkaline buffers (theoretical pH 9.8–10) without (left panel) and with (right panel) 20% (v/v) of glycerol. **a** Borate, **b** glycine, **c** carbonate–bicarbonate, **d** CAPS and **e** CHES. Spectra were shifted along Y-axis for better visualization. Measurements were performed under non-saturating conditions with microwave powers ranging from 2.4×10^{-3} to 1.9×10^{-2} mW

several alkaline buffers (theoretical pH of 9.8–10) at 10 K, without and with 20% (v/v) glycerol. In the absence of glycerol, the characteristic EPR signal attributable to the coordination of a hydroxide moiety to the ferric heme iron (LS state) is well

Table 1 Principal g values obtained by the simulations of CW X-band EPR spectra of myoglobin in different alkaline buffers without and with 20% glycerol (v/v). % contributions were determined by adding each species with its corresponding weight in the final simulation (weights determined using EasySpin software [29]).

	Species	g_x^{eff}	g_y^{eff}	g_z^{eff}	g_z	g_y	g_x	%
Without glycerol								
Borate	LS				2.619	2.157	1.836	100
Glycine	LS				2.624	2.159	1.836	100
Carbonate-bicarbonate	HS	5.910	5.910	2.002				100
CAPS	HS	5.910	5.910	2.002				2
	LS				2.602	2.175	1.843	98
CHES	HS	5.912	5.912	2.000				7
	LS				2.600	2.172	1.841	93
With 20% glycerol (v/v)								
Borate	HS	5.890	5.890	1.998				100
Glycine	LS				2.597	2.169	1.845	100
Carbonate-bicarbonate	HS	5.920	5.920	2.003				65
	LS				2.595	2.175	1.847	35
CAPS	HS	5.915	5.915	2.002				1
	LS				2.598	2.170	1.847	99
CHES	HS	5.910	5.910	1.998				2
	LS				2.595	2.170	1.846	98

Error margins: ± 0.005 for g values HS, ± 0.001 for g values LS, $\pm 1\%$ for contributions

resolved in all samples (principal g values are reported in Table 1), with the exception of the carbonate–bicarbonate buffer, where only the typical EPR signature of aquomet-myoglobin is detected (high-spin (HS) heme iron ($S = 5/2$)). In addition, in samples prepared in CAPS and CHES buffers, a minor contribution due to the HS state can be seen, though accounting for only less than 10% of the total spectrum. Already in the samples without glycerol, the EPR spectra vary both in HS/LS ratio and in principal g values of the LS species (Table 1). When glycerol is added to the sample, the expected narrowing of the signals of the LS form occurs due to the reduced mechanical stress on the biological molecule resulting from a better glass formation upon freezing, but also other changes are observed for some of the buffers indicating the non-innocent role of this cryoprotectant. The strongest and most unexpected effect is clearly observed in the spectrum of myoglobin in borate buffer. Here, the alkaline species completely reverts to the high-spin signal. Furthermore, a small but non-negligible change in the principal g values of the LS species—as well as a reduction in linewidth—is observed in the spectrum of myoglobin prepared in glycine buffer plus glycerol (Fig. 1b and Figure S1, Table 1). In the case of the carbonate–bicarbonate buffer, a small signal (~30%) from the OH^--ligated LS species can be detected upon the addition of the cryoprotectant (Fig. 1c and Figure S2, Table 1). Finally, when glycerol is present in the samples prepared in CAPS and CHES buffers, the contribution of the HS species is further diminished to 1–2% and the linewidth of the EPR signature of the LS species is reduced (Fig. 1d, e, Table 1).

Given the unexpected impact of glycerol in the measurements performed, the question is whether this effect is reproduced using alternative cryoprotectants. From Fig. 1 it follows that the borate and CAPS buffers yield, respectively, the highest and lowest change upon addition of glycerol. Figure 2 highlights the comparison between the X-band CW-EPR spectra of frozen solutions of ferric myoglobin prepared in borate and CAPS buffers, in the presence of 20% (v/v) glycerol, 20% (v/v) ethylene glycol, 0.36 M sucrose or 0.36 M trehalose. Clearly, all chosen glassing

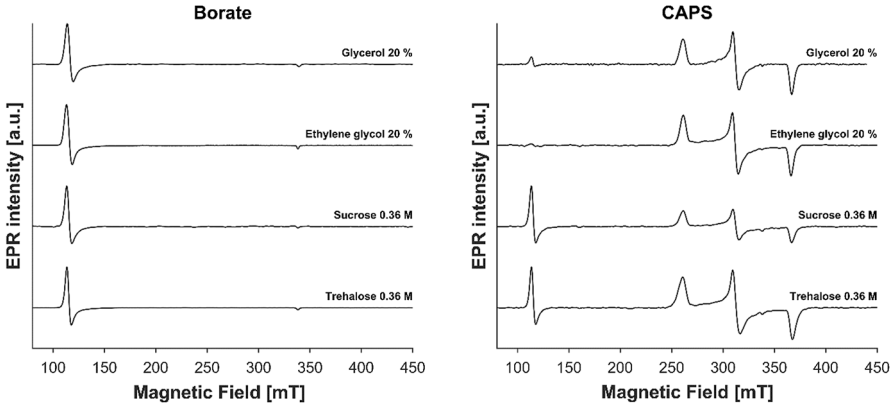

Fig. 2 X-band CW-EPR spectra of myoglobin in borate buffer (left panel) and CAPS buffer (right panel) in the presence of different cryoprotectants. Spectra were shifted along Y-axis for better visualization. Measurements were performed under non-saturating conditions with microwave powers in the range of 0.6–1.9 mW

agents prevent the formation of the LS OH^--ligated Mb adduct in the borate buffer (Fig. 2, left). In contrast, the LS contribution remains dominant independent of the cryoprotectant used for the CAPS buffer, even though the HS to LS ratio is not constant in the different samples (Fig. 2, right, principal g values are reported in Table 2).

Finally, the cryoprotectants were tested for their effectiveness as glassing agents, by comparing the CW-EPR linewidth of the OH^- ligated myoglobin and the 2-pulse echo decay. In the case of glycine, CAPS and CHES buffers, the CW-EPR spectra of myoglobin in presence of the chosen cryoprotectants show clear differences in spectral linewidth. In particular, the narrowest lines are obtained with ethylene glycol, followed—in order—by glycerol, sucrose and trehalose (Fig. 3 and Figure S3). For the samples prepared in carbonate–bicarbonate buffer, only glycerol and ethylene glycol allow the formation of the OH^--ligated LS species to some extent, while the addition of sucrose or trehalose does not cause any significant change from the sample prepared without cryoprotectant (Figure S4). The CW-EPR results are furthermore corroborated by the differences observed in the exponential decay of a two-pulse electron spin echo (Fig. 4), measured at the magnetic field position agreeing with $g = g_z$ for the sample of myoglobin in CAPS buffer with the different cryoprotectants. The T_m values obtained from curve-fitting (Figure S5) are presented in Table S1. The highest T_m, which reflects the narrowest line in the CW-EPR, is given by the addition of ethylene glycol. On the opposite side, sucrose appears to be the least efficient glassing agent, different from what is observed in the CW-EPR spectrum, where the least resolved line is given by trehalose.

In an attempt to better understand the effects observed in the EPR spectrum and relate them to concomitant effects on pH, freezing or interaction with the heme iron, samples of ferric myoglobin in the different alkaline buffers without or in presence of cryoprotectant were investigated at room temperature by means

Table 2 Principal g values obtained by the simulations of CW X-band EPR spectra of myoglobin in Borate and CAPS buffers in presence of alternative cryoprotectants % contributions were determined by adding each species with its corresponding weight in the final simulation (weights determined using EasySpin software [29])

	Species	g_x^{eff}	g_y^{eff}	g_z^{eff}	g_z	g_y	g_x	%
Borate								
Ethylene glycol 20%	HS	5.911	5.911	1.999				100
Sucrose 0.36 M	HS	5.910	5.910	2.000				100
Trehalose 0.36 M	HS	5.910	5.910	2.000				100
CAPS								
Ethylene glycol 20%	LS				2.588	2.167	1.846	100
Sucrose 0.36 M	HS	5.910	5.910	2.001				11
	LS				2.590	2.167	1.844	89
Trehalose 0.36 M	HS	5.910	5.910	2.000				5
	LS				2.597	2.166	1.840	95

Error margins: ± 0.005 for g values of HS, ± 0.001 for g values of LS, ± 1% for contributions

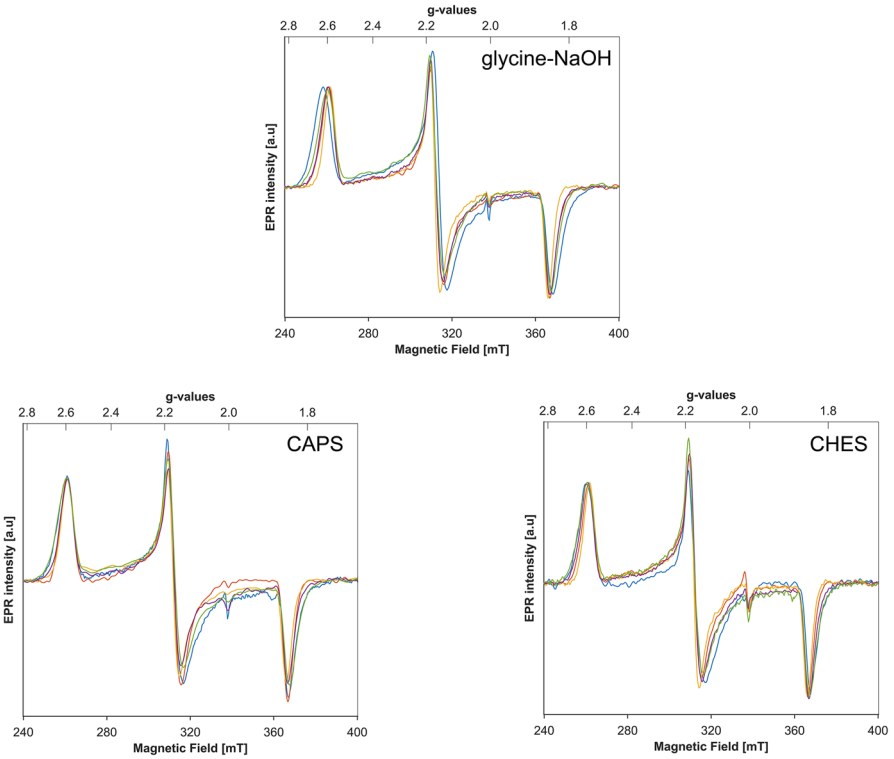

Fig. 3 X-band CW-EPR spectra of OH^--ligated LS of myoglobin samples prepared in glycine, CAPS and CHES buffer, respectively, in the presence of different glassing agents. Spectra were recorded under non-saturating conditions with a microwave power of ~ 0.3 mW. Plots are normalized at the centre of the g_z line. Cyan: no cryoprotectant added; red: 20% glycerol; dark yellow: 20% ethylene glycol; purple: 0.36 M sucrose; green: 0.36 M trehalose (color figure online)

of UV–visible absorption spectroscopy. As a reference, an additional sample of myoglobin was prepared in a HEPES buffer at pH 7. The obtained optical absorption spectra are depicted in Fig. 5. At neutral pH the typical bands of aquomet-myoglobin can be observed (Soret: 409 nm, Q-bands: 503 and 536 nm, charge transfer band: 636 nm), in good agreement with data reported in earlier studies [26, 30, 31]. The spectra of ferric myoglobin at alkaline pH present a red-shifted Soret peak (413 nm) with a shoulder at 483 nm and distinct Q-bands at 543 and 583 nm (shoulder at 593 nm). These features are independent of the chosen buffer and are consistent with a six-coordinated LS ferric heme iron [26, 31] deriving from the distal ligation of an OH^- group to the heme iron. Thus, it is clear that all the buffers selected for this work allow myoglobin to undergo an alkaline transition at room temperature. The addition of 20% (v/v) of glycerol induces evident spectral changes only in the sample prepared in borate buffer (Figure S7), where a mixture of contributions due to HS and LS species is detected. A similar result is obtained when ethylene glycol is added to the same buffer; however, there are

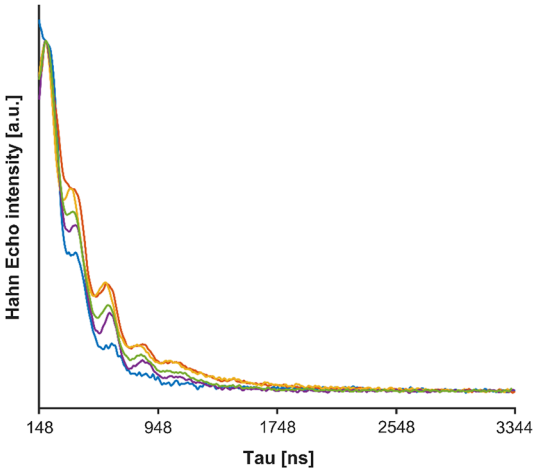

Fig. 4 X-band 2-pulse spin echo decay of myoglobin samples prepared in CAPS buffer with different cryoprotectants, measured at the g_z position. Cyan: no cryoprotectant added; red: 20% glycerol; dark yellow: 20% ethylene glycol; purple: 0.36 M sucrose; green: 0.36 M trehalose. Spectra were normalized at $\tau = 192$ ns. $t_{\pi/2}$ and t_{π} were adjusted for each sample to minimize the echo modulation. No cryoprotectant: 50/100 ns; 20% glycerol: 96/192 ns; 20% ethylene glycol: 96/192 ns; 0.36 M sucrose: 80/160 ns; 0.36 M trehalose: 96/192 ns. The differences in pulse length do not affect the spin echo decay (see Figure S6 for details) (color figure online)

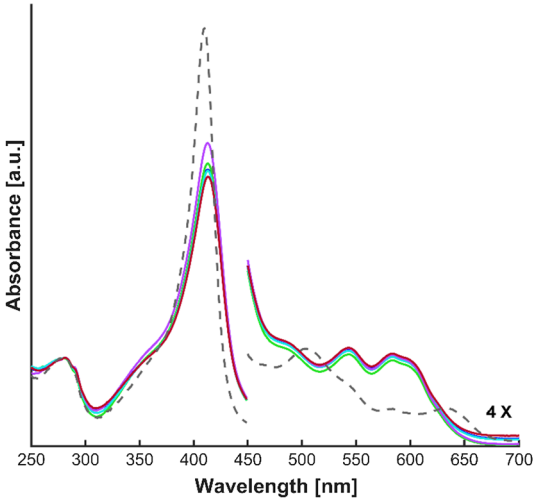

Fig. 5 UV–Vis absorption spectra of myoglobin in different buffers (theoretical pH 9.8–10) at room temperature. Blue: borate; green: glycine; cyan: carbonate–bicarbonate; purple: CAPS; red: CHES. The spectrum of myoglobin in 50 mM HEPES buffer pH 7 is reported in grey dashed line for comparison. For clarity, all the spectra are normalized to the absorption band at $\lambda = 280$ nm and inset is 4x-magnified (color figure online)

no visible changes in presence of sucrose or trehalose. Consistent with the EPR results, the UV–visible spectra of myoglobin in the other buffers are not affected by the addition of any of these compounds.

3.2 Buffering Capacity

EPR and UV–visible spectroscopy findings show that the pH of the selected buffers can be affected by either temperature or a direct interaction with the cryoprotectants. Table 3 (top section) reports the pH of the different buffers, measured at room temperature, when glycerol is added to different final concentrations. It can be seen that the pH of the borate buffer is strongly affected by the addition of glycerol, with a drop of 1.5 units in the presence of only 5% (v/v) of cryoprotectant and a further decrease until neutrality when glycerol is 30% (v/v). Nonetheless, the other buffers are not significantly influenced by the presence of this cryoprotectant. While carbonate appears to be the most stable, a decrease between 0.16 and 0.23 pH units in glycine, CAPS and CHES at the highest concentration of cryoprotectant could be attributed to the diminished buffering capacity due to dilution.

Next, the pH of the buffers was measured in presence of ethylene glycol (20% v/v), sucrose and trehalose (final concentration 0.36 M). The data in Table 3 (bottom section) show that even in presence of these glassing agents the pH of the borate buffer is not stable, though the change is not as dramatic as with glycerol. On the other side, the pH of the other buffers is not significantly affected by the addition of either sucrose, trehalose or ethylene glycol at room temperature.

4 Discussion

In this work, we observed the effects of particular combinations of buffer and cryoprotectant on the EPR spectra of myoglobin samples prepared at high pH. Our findings can be summarized as follows:

Table 3 pH changes of different alkaline buffers upon addition of glycerol and other cryoprotectants

% Glycerol (v/v)	pH				
	Borate	Glycine	Carbonate–bicarbonate	CAPS	CHES
0	9.99	9.92	9.96	9.88	10.13
5	8.69	9.92	9.96	9.85	10.11
10	8.11	9.86	9.96	9.79	10.08
15	7.75	9.83	9.96	9.74	10.05
20	7.48	9.80	9.96	9.70	10.02
30	7.04	9.75	9.96	9.65	9.97
Other glassing agents					
Buffer alone	10.00	10.40	10.36	9.80	10.53
20% ethylene glycol (v/v)	8.91	10.38	10.60	9.80	10.46
0.36 M sucrose	9.38	10.34	10.24	9.82	10.46
0.36 M trehalose	9.50	10.37	10.24	9.80	10.51

Error margin of ± 0.01 pH units

pH Effects. The first and plain observation is that a chemical reactivity with the cryoprotectant can substantially alter the pH of specific buffers, as it happens in the case of borate buffer. Boric acid is known to react with glycerol to form a boron–chelate complex, which increases the acidity of the solution [32, 33]. Our pH measurements are in good agreement with this evidence and demonstrate that this reaction can also occur, to a lesser extent, with different polyols such as ethylene glycol, sucrose and trehalose. When the pH is lowered from 10.0 to 8.91 in the presence of ethylene glycol (Table 3, bottom section), a mixture of high-spin and low-spin myoglobin is observed with UV–visible absorption spectroscopy. The minor decreases to 9.38 and 9.50, induced by sucrose and trehalose, still allow the protein to adopt a complete low-spin configuration (Figure S6), as expected from the known pKa value of the alkaline transition of myoglobin (~ 8.9) [19, 23, 24].

Temperature Effects. The EPR signals of the same samples were apparently inconsistent with UV–visible spectroscopy results, as we could not observe any LS OH^--ligated heme species no matter which cryoprotectant was added to the borate buffer (Fig. 2, left panel). This indicates an additional influence of temperature on the pH stability of this buffer, which could also explain the complete absence of the EPR signal due to the LS species in the spectrum of myoglobin in carbonate–bicarbonate buffer (Fig. 1c, left panel). The pH variation of common biological buffers upon freezing has been extensively described in the literature [34–36]. In particular, Orii and Morita, monitoring colour changes in pH-sensitives dyes, observed that even a minimum amount of glycerol (5%) caused the pH of borate buffer to decrease from 8.5 to a value between 6.3 and 6.8 at room temperature, but this effect was dramatically enhanced by freezing, since they measured a pH drop to a value of 2–3. The same authors reported a similar evidence with a carbonate–bicarbonate buffer, whose pH was observed to decrease of more than 3 units upon freezing. Nonetheless, the addition of glycerol to this buffer had the opposite effect, as it was able to inhibit the pH drop to some extent [34]. The latter observation is consistent with the presence of a minor contribution from the OH^- LS species in the spectrum of myoglobin in the carbonate–bicarbonate buffer when 20% (v/v) of glycerol or ethylene glycol is added to the sample (Fig. 1c, right panel and Figure S2). Finally, a temperature effect on CAPS and CHES buffers, though less severe in comparison with the above-mentioned buffers, should not be excluded. This speculation is supported by the presence of a residual HS signal in these samples (Fig. 1d, e, left panel) which suggests a modest pH decrease at the cryogenic temperature. It has been reported that the pH of CAPS can decrease about 1 unit upon freezing, opposite to other Good's buffers, which tend to increase their pH [34, 37]. Our findings suggest that the decrease in pH for CHES is even more pronounced than for CAPS; however, to our knowledge no information is reported about this particular buffer system.

Interactions with the Protein. On a different note, the chemical structure of the buffer molecule and its physical interactions either with the protein moiety or with the cryoprotectant might be responsible for some observations in the EPR spectra of the samples prepared in glycine and borate buffers. Being small molecules, glycine and borate can likely enter the heme pocket of myoglobin and both are expected to be mainly negatively charged at pH ~ 10 (pKa of glycine α-amino group ~ 9.6 [38], pKa of boric acid ~ 9.24 [39]). Therefore, it is possible that some

of these charged molecules sitting close to the heme would influence the overall electronic distribution of the spin system, even without directly coordinating the iron [40], which would probably result in a consistent variation of the g values. In the EPR spectra of myoglobin in glycine buffer, a reduction in the $\boldsymbol{g}$ anisotropy occurs if any of the cryoprotectants is added, with the major shift observed in presence of ethylene glycol (Fig. 3, S1 and S3). Moreover, in the absence of cryoprotectant, the g values of alkaline myoglobin in the glycine buffer are similar to the ones of the sample prepared in the borate buffer, but differ from the ones of samples prepared in CAPS or CHES (Table 1), which is consistent with the latter being bigger molecules unable to approach the heme site. The small variations in the g values could be also attributed to a change in the dielectric constant of the solvent, a factor which could be likely affected by the addition of a cryoprotectant.

Effectiveness of the Cryoprotectant. Finally, we evaluated the efficiency of the chosen cryoprotectants as actual glassing agents. To do so, we first compared the linewidth of the OH^- low-spin features in the myoglobin samples prepared in presence of the different cryoprotectants (Fig. 3 and S3). A trend can be recognized for all the tested buffers, where ethylene glycol gives the most resolved signals, followed by glycerol and sucrose which have similar effects. When trehalose is employed, the strain is greater and close to the sample prepared in the absence of cryoprotectant, indicating the poor efficacy of this substance as a glassing agent, notwithstanding its structure being similar to sucrose. Phase memory times measurements are in line with CW-EPR results, pointing out ethylene glycol as the most effective cryoprotectant, in terms of glass formation, among the substances employed in this study.

5 Conclusions

In spectroscopic experiments, it is crucial to distinguish the results attributable to a certain experimental condition from those due to the intrinsic properties of the examined system. This work is intended to highlight the need of tailoring the procedural setup when performing EPR experiments on (heme) proteins, to identify possible artefacts. To this regard, by investigating the well-characterized myoglobin, we show a non-negligible relationship between multiple external factors such as pH, buffer composition, temperature and the addition of a cryoprotectant to the sample. Notably, our results corroborate many effects already observed and reported scattered in literature, but insufficiently tested in a systematic way in the context of EPR spectroscopy. In brief, we show that (i) borate buffer has a propensity to react with glycerol and polyols in general with a consequent lowering of the pH, so it should be avoided if such cryoprotectants are needed; (ii) some high-pH buffers, such as carbonate–bicarbonate buffer, undergo dramatic pH change upon freezing, preventing the observation of expected alkaline transitions; (iii) small buffer molecules can affect the heme environment as it happens in the case of glycine and borate; (iv) in the chosen set of cryoprotectants, ethylene glycol forms the best glass for low-temperature EPR experiments.

Supplementary Information The online version contains supplementary material available at https://doi.org/10.1007/s00723-021-01428-w.

Acknowledgements The authors would like to acknowledge the use of Servicio General de Apoyo a la Investigación-SAI, Universidad de Zaragoza.

Author contribution Not applicable/relevant.

Funding This paper is part of a project that has received funding from the European Union's Horizon 2020 research and innovation program under the Marie Skłodowska-Curie grant agreement No. 813209.

Code Availability Upon acceptance, data and simulations script will be available at https://zenodo.org/communities/paracat_community/?page=1&size=20

Declarations

Conflict of interest The authors declare no conflict of interest.

Ethical Approval Not applicable/relevant.

Consent to Participate Not applicable/relevant.

Consent for Publication Not applicable/relevant.

References

1. W.B. Mims, J. Peisach, in *Biological Magnetic Resonance*, vol. 3, ed. by L.J. Berliner, J. Reuben (Plenum Press, New York, 1981), pp. 213–263
2. J. Dubochet, M. Adrian, J.-J. Chang, J. Lepault, A.W. McDowall, in *Cryotechniques in Biological Electron Microscopy*. ed. by R.A. Steinbrecht, K. Zierold (Springer, Berlin Heidelberg, 1987), pp. 114–131
3. P. Brüggeller, E. Mayer, Nature **288**, 569 (1980)
4. D.S. Russell, *Physical Methods for Chemists*, 2nd edn. (Surfside Scientific Publishers, Gainesville, 1992)
5. A.R. Bizzarri, S. Cannistraro, Eur. Biophys. J. **22**, 259 (1993)
6. J.R. Brender, S. Kishimoto, G.R. Eaton, S.S. Eaton, Y. Saida, J. Mitchell, M.C. Krishna, Magn. Reson. Med. **85**, 42 (2021)
7. P.M.A. Gadsby, J. Peterson, N. Foote, C. Greenwood, A.J. Thomson, Biochem. J. **246**, 43 (1987)
8. T. Yonetani, H. Anni, J. Biol. Chem. **262**, 9547 (1987)

9. G. Smulevich, A.R. Mantini, A.M. English, J.M. Mauro, Biochemistry **28**, 5058 (1989)
10. J.H.A. Nugent, Biochim. Biophys. Acta Bioenerg. **1504**, 288 (2001)
11. C.J. Halkides, C.T. Farrar, D.J. Singel, J. Magn. Reson. **134**, 142 (1998)
12. E.R. Georgieva, A.S. Roy, V.M. Grigoryants, P.P. Borbat, K.A. Earle, C.P. Scholes, J.H. Freed, J. Magn. Reson. **216**, 69 (2012)
13. C.G. Hoogstraten, R.D. Britt, RNA **8**, 252 (2002)
14. S.K. Chapman, S. Daff, A.W. Munro, in *Metal Sites in Proteins and Models. Structure and Bonding*, vol. 88, ed. by H.A.O. Hill, P.J. Sadler, A.J. Thomson (Springer, Berlin Heidelberg, 1997), pp. 39–70
15. M.A. Liebert, M. Paoli, J.O.N. Marles-wright, A.N.N. Smith, DNA Cell Biol. **21**, 271 (2002)
16. D. Goldfarb, S. Stoll, *EPR Spectroscopy: Fundamentals and Methods* (Wiley, 2018)
17. B. Garcia-Moreno, J. Biol. **8**, 98 (2009)
18. M.V. Arbige, J.K. Shetty, G.K. Chotani, Trends Biotechnol. **37**, 1355 (2019)
19. D.A. Svistunenko, M.A. Sharpe, P. Nicholls, C. Blenkinsop, N.A. Davies, J. Dunne, M.T. Wilson, C.E. Cooper, Biochem. J. **351**, 595 (2000)
20. F.P. Nicoletti, J.P. Bustamante, E. Droghetti, B.D. Howes, M. Fittipaldi, A. Bonamore, P. Baiocco, A. Feis, A. Boffi, D.A. Estrin, G. Smulevich, Biochemistry **53**, 8021 (2014)
21. D.L. Brautigan, B.A. Feinberg, B.M. Hoffman, E. Margoliash, J. Peisach, W.E. Blumberg, J. Biol. Chem. **252**, 574 (1977)
22. B.R. Streit, B. Blanc, G.S. Lukat-Rodgers, K.R. Rodgers, J.L. Dubois, J. Am. Chem. Soc. **132**, 5711 (2010)
23. P. George, G. Hanania, Biochem. J. **52**, 517 (1952)
24. M. Brunori, G. Amiconi, E. Antonini, J. Wyman, R. Zito, A. Rossi Fanelli, BBA Protein Struct. **154**, 315 (1968)
25. D.A. Svistunenko, B.J. Reeder, M.M. Wankasi, R.L. Silaghi-Dumitrescu, C.E. Cooper, S. Rinaldo, F. Cutruzzolà, M.T. Wilson, Dalt. Trans. **8**, 840 (2007)
26. O. Baffa, O.R. Nascimento, M. Tabak, Biochim. BBA Protein Struct. **832**, 63 (1985)
27. W.J. Bowen, J. Biol. Chem. **179**, 235 (1949)
28. E. Antonini, M. Brunori, *Hemoglobin and Myoglobin in Their Reactions with Ligands* (North-Holland publishing Co., Amsterdam, 1972)
29. S. Stoll, A. Schweiger, J. Magn. Reson. **178**, 42 (2006)
30. L. Tofani, A. Feis, R.E. Snoke, D. Berti, P. Baglioni, G. Smulevich, Biophys. J. **87**, 1186 (2004)
31. W.A. Eaton, R.M. Hochstrasser, J. Chem. Phys. **49**, 985 (1968)
32. A.Z. Halimehjani, H. Gholami, M.R. Saidi, Green Chem. Lett. Rev. **5**, 1 (2012)
33. C. Mukhopadhyay, A. Datta, R.J. Butcher, Tetrahedron Lett. **50**, 4246 (2009)
34. Y. Orii, M. Morita, J. Biochem. **81**, 163 (1977)
35. D.L. Williams-Smith, R.C. Bray, M.J. Barber, A.D. Tsopanakis, S.P. Vincent, Biochem. J. **167**, 593 (1977)
36. N. Le Breton, J.J. Wright, A.J.Y. Jones, E. Salvadori, H.R. Bridges, J. Hirst, M.M. Roessler, J. Am. Chem. Soc. **139**, 16319 (2017)
37. L. Veselý, B. Susrisweta, D. Heger, Int. J. Pharm. **593**, 120128 (2021)
38. M.J. O'Neil, *The Merck Index: An Encyclopedia of Chemicals, Drugs, and Biologicals*, 15th edn. (Royal Society of Chemistry, 2013)
39. D. Schubert, *Kirk-Othmer Encyclopedia of Chemical Technology* (Wiley, New York, 2011)
40. P. Bernal Bayard, L. Puerto Galán, I. Yruela Guerrero, I. García Rubio, M.C. Castell, J.M. Ortega, P.J. Alonso, M. Roncel, J.I. Martínez, M. Hervás, J.A. Navarro, Photosynth. Res. **133**, 273 (2017)

Authors and Affiliations

Ilenia Serra[1,2] · Inés García Rubio[2,3] · Sabine Van Doorslaer[1]

Ilenia Serra
Ilenia.Serra@uantwerpen.be

[1] BIMEF Laboratory, Department of Chemistry, University of Antwerp, 2610 Antwerp, Belgium

[2] Department of Condensed Matter Physics, Faculty of Sciences, University of Zaragoza, 50009 Zaragoza, Spain

[3] Centro Universitario de la Defensa, 50090 Zaragoza, Spain